

Chaotic response of the 2D semi-geostrophic and 3D quasi-geostrophic equations to gentle periodic forcing *

Dorian Goldman [†] and Robert J. McCann [‡]

May 10, 2008

Abstract

Symmetries and Hamiltonian structure are combined with Melnikov's method to show a set of exact solutions to the 2D semi-geostrophic equations in an elliptical tank respond chaotically to gentle periodic forcing of the domain eccentricity (or of the potential vorticity, for that matter) which are sinusoidal in time with nearly any period. A similar approach confirms the chaotic response of the quasi-geostrophic equations to gentle periodic forcing by an external shearing field. Our approach simplifies and strengthens the proof by Bertozzi (upon which it is based) concerning the chaotic response of Kirchoff elliptical vortex patches to gentle shearing in the 2D Euler equations.

Introduction

The semi-geostrophic approximation from meteorology and oceanography is sometimes used to study the large-scale, long-time dynamics of a stratified rotating fluid. Numerical studies suggest it predicts dynamics less turbulent [6], [7], [8] than those of the primitive equations of hydrodynamics from which it is derived, which Cullen [7] highlights as an attractive feature of the semi-geostrophic model. It is therefore natural to wonder whether this approximation precludes some of the chaotic behavior associated with other atmospheric models [12], [22] and idealized problems in fluid mechanics [1], [3].

In this paper we provide some mathematical evidence to the contrary. The semi-geostrophic equations are introduced as an approximation of the 2D incompressible Euler equations, and a set of exact solutions to these equations is presented from [20] corresponding to the case that the fluid occupies an elliptical tank. This is done in section 2. The resulting dynamics end up resembling

*©2007 by the authors. Reproduction of this article, in its entirety, is permitted for noncommercial purposes. To appear in *Nonlinearity*.

[†]Department of Mathematics, University of Toronto, Toronto, Ontario M5S2E4, Canada

[‡]Department of Mathematics, University of Toronto, Toronto, Ontario M5S3G3, Canada

a more complicated variant of the dynamics of the Kirchoff ellipse, which was first analyzed by Kirchoff [19], and subsequently by Kida [18], Neu [26], Bertozzi [3], Meacham et al [25] and others, but with potential vorticity playing the role vorticity plays in the 2D Euler equations. In fact, by using a slightly simpler argument than in [3], it is shown that under small perturbations of the elliptical tank's eccentricity, that the equations from [20] evolve chaotically. This is accomplished by using the Melnikov method [24], whose origins can already be discerned in the celebrated work of Poincaré [27]. We direct the interested reader to [17] for the historical development and a thorough treatment of the Melnikov method. This method provides a computational way of determining when a dynamical system is chaotic by exploiting the Smale-Birkhoff theorem, which was anticipated by Birkhoff [4] and established rigorously by Smale [29]. It provides sufficient conditions for the neighborhood around a homoclinic orbit of a dynamical system to possess a chaotic subsystem.

For the Kirchoff ellipse, Bertozzi [3] used the non-Hamiltonian form of the Melnikov method [24] to prove the dynamics evolve chaotically under perturbations by a shearing flow. We show that except for one parameter value, the dynamics of the Kirchoff ellipse can also be modeled using the homoclinic orbit of a Hamiltonian system, hence a somewhat simpler calculation yields essentially the same result. We also extend the range of perturbation frequencies which result in chaotic dynamics to all but a countable, topologically isolated set, which improves Bertozzi's result on the existence of an interval of such frequencies. Our method of proof relies on exploiting symmetries in two degree of freedom Hamiltonian systems, along with the analyticity of the Fourier transform of a rapidly decaying function, in order to simplify the Melnikov analysis. Our method is similar to the method employed by Dankowicz and Holmes and Holmes and Marsden in the context of the Sitnikov [10] and asymmetric central forcing problems [16]. Similar results for the quasi-geostrophic equations are derived by Meacham et al [25] by applying Melnikov analysis to ellipsoidal vortices in a shearing field and by Meacham et al [22] for the quasi-geostrophic ellipsoidal vortex patch, but by using a computational approach to infer chaotic dynamics when a non-divergent unidirectional vertical shearing is perturbed periodically. Cullen and Douglas [9] show using rearrangement methods that solutions of the semi-geostrophic equations are unstable for large values of inverse potential vorticity (defined in section 2). Our result provides an independent way of verifying instability of the semi-geostrophic equations within this regime. We also provide an analytical method of evaluating the Melnikov integral under gentle periodic forcing of the quasi-geostrophic model by a horizontal shearing field, similar to our approach to the 2D Euler equation and semi-geostrophic model. Some motivation for the problem is given in section 3 along with the proofs of the propositions.

1 Chaos and Nonlinear Dynamics

1.1 Dynamical systems. In this section we review some well-known results from the theory of chaotic dynamics focusing our attention, for simplicity, on a smooth planar autonomous Hamiltonian vector field $H : \Omega \subset \mathbf{R}^2 \rightarrow \mathbf{R}$,

$$\dot{\mathbf{x}} = J\nabla H(\mathbf{x}) = \mathbf{f}(\mathbf{x}) \quad (1)$$

where

$$J := \begin{pmatrix} 0 & -1 \\ 1 & 0 \end{pmatrix} \quad (2)$$

and a dot denotes $\frac{d}{dt}$. Recall that a *fixed point* of (1) is a point $\mathbf{x}_0 \in \Omega$ such that $\mathbf{f}(\mathbf{x}_0) = 0$. We say this fixed point is *hyperbolic* if $D\mathbf{f}(\mathbf{x}_0)$ has two linearly independent eigenvectors $\mathbf{e}_1, \mathbf{e}_2$ corresponding to eigenvalues with non-zero real part. In our case there will always be one positive and one negative eigenvalue α^+ and α^- corresponding to \mathbf{e}_1 and \mathbf{e}_2 respectively with $\alpha^\pm = \pm\alpha$ due to the Hamiltonian structure of the vector field. A *saddle connection* between two hyperbolic fixed points is a curve $\mathbf{q}_0 : \mathbf{R} \rightarrow \mathbf{R}^2$ with continuous extension to $\mathbf{R} \cup \{\pm\infty\}$, such that $\mathbf{q}_0(\infty) = \mathbf{p}_1$ and $\mathbf{q}_0(-\infty) = \mathbf{p}_2$, which satisfies (1) for all $t \in \mathbf{R}$. The saddle connection, and the fixed points $\mathbf{p}_1, \mathbf{p}_2$ are called *homoclinic* when $\mathbf{p}_1 = \mathbf{p}_2$ and *heteroclinic* otherwise (see Figure 3 for an example of a homoclinic saddle connection). For a continuous dynamical system of the form (1), we can construct the *Poincaré map* by extending our phase space to include time as a dimension, $\Omega \times \mathbf{R}$, and consider the intersection of the orbit $(\mathbf{q}_0(t), t)$ with planes $t_n = t_0 + nT$ for $n \in \mathbf{N}$, projected back onto $t = t_0$ (see Figure 1). This yields an iterative map, $\mathbf{P} := \mathbf{P}_{t_0} : \Omega \rightarrow \Omega$. We also say that \mathbf{q} is a fixed point of \mathbf{P} if $\mathbf{P}(\mathbf{q}) = \mathbf{q}$. We then say that this map has a *hyperbolic* fixed point at \mathbf{q} if $D\mathbf{P}(\mathbf{q})$ has two linearly independent eigenvectors $\mathbf{e}_1, \mathbf{e}_2$ corresponding to eigenvalues $\lambda_1 > 1$ and $1 > \lambda_2 > 0$. The map \mathbf{P} is a diffeomorphism and (Ω, \mathbf{P}, d) , where d denotes the standard euclidian distance, is a discrete time dynamical system. For a fixed point \mathbf{q} of \mathbf{P} , we can then naturally define the stable, and unstable manifolds,

$$W^s(\mathbf{q}) = \{\mathbf{x} \in \Omega \mid \mathbf{P}^n(\mathbf{x}) \rightarrow \mathbf{q} \text{ as } n \rightarrow \infty\} \quad (3)$$

$$W^u(\mathbf{q}) = \{\mathbf{x} \in \Omega \mid \mathbf{P}^n(\mathbf{x}) \rightarrow \mathbf{q} \text{ as } n \rightarrow -\infty\} \quad (4)$$

We say the manifolds W^s and W^u of the fixed point \mathbf{q} intersect *transversally* if $\dim\{\text{span}(T_s, T_u)\} = \dim T_u + \dim T_s = 2$ where T_s, T_u denote the tangent spaces of W^s and W^u respectively at the point of intersection.

1.2 The bi-infinite shift on 2 symbols. Let

$$\Sigma_2 = \{s = (\cdots, s_{-2}, s_{-1}, s_0, s_1, s_2, \cdots) \mid s_i = 1, 0\}. \quad (5)$$

We can define a metric $d(s, t) = \sum_{i=-\infty}^{\infty} \frac{1}{2^{|i|}} |s_i - t_i|$ that turns (Σ_2, d) into a topological space. The *shift map*, $\sigma : \Sigma_2 \rightarrow \Sigma_2$ defined by $(\sigma(s))_i = s_{i+1}$

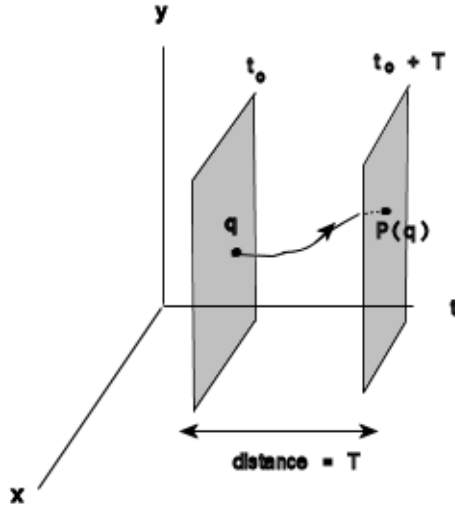


Figure 1: Forward iteration of Poincaré map, $P_{t_0} := P$ in figure. The point q gets mapped to $P(q)$ where it intersects the next plane.

turns (Σ_2, d, σ) into a discrete dynamical system. This dynamical system has an infinite number of periodic orbits with arbitrarily long periods and sensitive dependence on initial conditions (see [11]). Since the shift dynamics (Σ_2, d, σ) satisfy any reasonable definition of chaos, one way to establish the presence of chaos in our systems is to show that each of them contains a subsystem on which the dynamics are topologically conjugate to those of (Σ_2, d, σ) . For our purposes we will say a dynamical system (Ω, d, \mathbf{P}) is chaotic if it is topologically conjugate to (Σ_2, d, σ) . The following theorem anticipated by Birkhoff [4] and established by Smale [29] provides sufficient conditions for a dynamical system to contain a chaotic subsystem.

Theorem 1 (Smale, Birkhoff) *Suppose $\mathbf{P}: \Omega \rightarrow \Omega \subset \mathbf{R}^2$ is a diffeomorphism with a hyperbolic fixed point \mathbf{p} whose stable and unstable manifolds intersect transversally at \mathbf{q} . Then some iterate \mathbf{P}^n has an set I on which it is topologically equivalent (conjugate) to the bi-infinite shift on two symbols.*

1.3 Melnikov's Method. The problem now is to determine sufficient conditions for such transversal intersections of the stable and unstable manifolds to occur. Melnikov [24] stated the following sufficient condition for an unperturbed vector field with a homoclinic saddle connection (see figure 3) to possess time periodic perturbations for which the stable and unstable manifolds of the perturbed Poincaré map intersect transversally, to leading order in the perturbation. As in Wiggins [31] we consider a time periodic perturbation of (1) of

the form,

$$\dot{\mathbf{x}} = \mathbf{f}(\mathbf{x}) + \epsilon \mathbf{g}(\mathbf{x}, t, \epsilon), \quad (6)$$

$$\text{where } \mathbf{g}(\mathbf{x}, t + T, \epsilon) = \mathbf{g}(\mathbf{x}, t, \epsilon)$$

for some $T > 0$. We define the Melnikov integral for planar Hamiltonian vector fields,

$$M(t_0) = \int_{-\infty}^{\infty} \mathbf{f}(\mathbf{q}_0(t)) \wedge \mathbf{g}(\mathbf{q}_0(t), t + t_0, 0) dt \quad (7)$$

where $\mathbf{q}_0(t)$ denotes the parameterized homoclinic saddle connection between of a hyperbolic fixed point of the unperturbed system and \wedge is the wedge product, defined as $\mathbf{a} \wedge \mathbf{b} = a_1 b_2 - a_2 b_1$. We state Melnikov's Theorem.

Theorem 2 (Melnikov): *Given that $\mathbf{f} \in C^r(\Omega; \mathbf{R})$, $\mathbf{g} \in C^r(\Omega \times \mathbf{R}^2; \mathbf{R})$ where $\Omega \subset \mathbf{R}^2$ for $r \geq 2$, \mathbf{g} has a C^2 dependence on ϵ , and for $\epsilon = 0$, (6) possesses a homoclinic saddle connection with hyperbolic fixed point \mathbf{p} . If there exists a $t_0 \in \mathbf{R}$ such that $M(t_0) = 0$ and $M'(t_0) \neq 0$ (called a simple zero in [24]), then $W^s(\mathbf{p}_\epsilon)$ and $W^u(\mathbf{p}_\epsilon)$ intersect transversally for $\epsilon > 0$ sufficiently small, where \mathbf{p}_ϵ is a fixed point of the time T -Poincaré map P_T^ϵ .*

The proof of the above theorem and derivation of the Melnikov integral is well known and can be found in [11], [17], [31].

We now introduce some exact solutions to the 2D Semi-Geostrophic equations developed by McCann and Oberman [20]. The following section is devoted to these. In section 3, the results of this section are used to demonstrate chaotic dynamics are present under perturbations of the vector field appropriate for the use of Melnikov's theorem.

2 Some exact solutions to the semi-geostrophic (SG) and quasi-geostrophic (QG) equations

2.1 Derivation of SG from 2D Euler equations. The 2D incompressible Euler equations on a bounded domain $Y \subset \mathbf{R}^2$ with rotating frame of reference and unit density are

$$(\partial_t + \mathbf{v} \cdot \nabla)\mathbf{v} + 2\Omega J\mathbf{v} = -\nabla P \quad (8)$$

$$\nabla \cdot \mathbf{v} = 0, \quad (9)$$

$$\mathbf{v} \cdot \hat{\mathbf{n}} = 0, \quad (10)$$

where $\hat{\mathbf{n}}$ is the normal to the boundary Y , and \mathbf{v} is a function of space and time, so $\mathbf{v} : Y \times [0, \infty) \rightarrow \mathbf{R}^2$. The symplectic matrix J is defined as in (2), and we choose units of time so that $2\Omega = 1$.

These equations can be re-written in terms of a stream function since the incompressibility condition yields

$$\mathbf{v}(\mathbf{x}, t) = J\nabla\psi(\mathbf{x}, t). \quad (11)$$

The Euler equations then become:

$$\nabla \frac{\partial\psi}{\partial t} + (D^2\psi + I)J\nabla\psi - J\nabla P = 0. \quad (12)$$

In large scale atmospheric flow, the acceleration terms in the Euler equations can be neglected entirely which gives $\psi = P$. This is called the *geostrophic approximation*. We therefore call the quantity $J\nabla P$ the *geostrophic velocity* (as opposed to the full velocity $J\nabla\psi$). The *semi-geostrophic* approximation to the Euler equations involves approximating the small terms only in (12) by $\psi \sim P$ so that we get

$$\nabla \frac{\partial P}{\partial t} + (D^2P + I)J\nabla\psi - J\nabla P = 0. \quad (13)$$

The semi-geostrophic equations satisfy conservation of *potential vorticity*, $1/\lambda(\mathbf{y}, t)$ defined by,

$$\frac{1}{\lambda^2} := \det[I + D^2P(t, \mathbf{y})] \quad (14)$$

in much the same way vorticity, $\text{trace}(I + D^2\psi)$ is conserved along lagrangian particle trajectories in the 2D Incompressible Euler equations. The *quasi-geostrophic* approximation to the Euler equations involves replacing the coefficient $J\nabla\psi$ of D^2P with $J\nabla P$ in equation (13), and takes the form,

$$\nabla \frac{\partial P}{\partial t} + D^2P J\nabla P + J\nabla\psi - J\nabla P = 0. \quad (15)$$

2.2 Exact solutions when Y is an ellipse McCann and Oberman [20] considered the fluid restricted to an elliptical tank, so that the domain Y in the above equations is a fixed ellipse, with the evolution considered under the SG approximation given by (13). Following Cullen and Purser [5], they define $V(t, \mathbf{y}) := P(t, \mathbf{y}) + \frac{1}{2}(\mathbf{y}^T \cdot \mathbf{y})$ and introduce the Legendre transform of $V(t, \mathbf{y})$,

$$U(t, \mathbf{x}) = \sup_{\mathbf{y} \in Y} \mathbf{y}^T \cdot \mathbf{x} - V(t, \mathbf{y}),$$

with

$$\begin{aligned} \rho(t, \mathbf{x}) &:= \det D^2 U(t, \mathbf{x}), \\ \nabla U(t, \mathbf{R}^2) &\subset \tilde{Y}, \end{aligned}$$

and $\rho(t, \mathbf{x})$ defined as the *inverse potential vorticity* which is conserved along lagrangian particle trajectories. This conservation law tells us that ∇V maps Y to a *dynamical inverse potential vortex patch* $X(t)$ of constant intensity (similar to the elliptical vortex patch studied in [3]), which is shown to also be an ellipse at all times by verifying consistency of the ansatz that $P(t, \mathbf{y})$ and $Q(t, \mathbf{y})$ remain quadratic functions of space at each instant in time. They then show the evolution can be reduced to an ordinary differential equation in these *dual* coordinates, $a(t)$ and $\tilde{\theta}(t)$ representing the aspect ratio and inclination of the ellipse $X(t)$ with respect to the x -axis. Cast into canonically conjugate variables, $r = (a + 1/a)/2$ and expressing $s = \cosh(\varphi) \geq 1$, they obtain a Hamiltonian system, which we will express in coordinates $(r, \theta := 2\tilde{\theta})$ which for our purposes, are more convenient than those of [20]. These coordinates reveal the homoclinic orbits in our phase space more readily and allow for comparison to the vortex patch solutions of the 2D Euler and QG equations. The equations for the evolution of the dual ellipse in these coordinates are,

$$\frac{d}{dt} \begin{pmatrix} r \\ \theta \end{pmatrix} = J \nabla H_{SG}^{\lambda, s}(r, \theta), \quad (16)$$

$$\frac{H_{SG}^{\lambda, s}}{2}(r, \theta) = \lambda^2 s + r - \lambda \left(2 + 2rs + 2 \cos \theta \sqrt{(r^2 - 1)(s^2 - 1)} \right)^{1/2}, \quad (17)$$

$$\varphi < \varphi_{cr}(\lambda), \quad \lambda > 2$$

here λ is a constant defined by (14), e^φ represents the aspect ratio of the physical domain Y and $\varphi_{cr}(\lambda)$ is defined by (18) (discussed further below). We note that the above Hamiltonian is still well defined for all positive values of φ and λ , and the Cullen and Purser stability criterion continues to be satisfied for all of the McCann and Oberman solutions which satisfy it initially. However there is no homoclinic orbit when $\varphi \geq \varphi_{cr}(\lambda)$ and hence one cannot employ Melnikov analysis to establish the existence of chaotic dynamics.

2 SOME EXACT SOLUTIONS TO THE SEMI-GEOSTROPHIC (SG)
AND QUASI-GEOSTROPHIC (QG) EQUATIONS

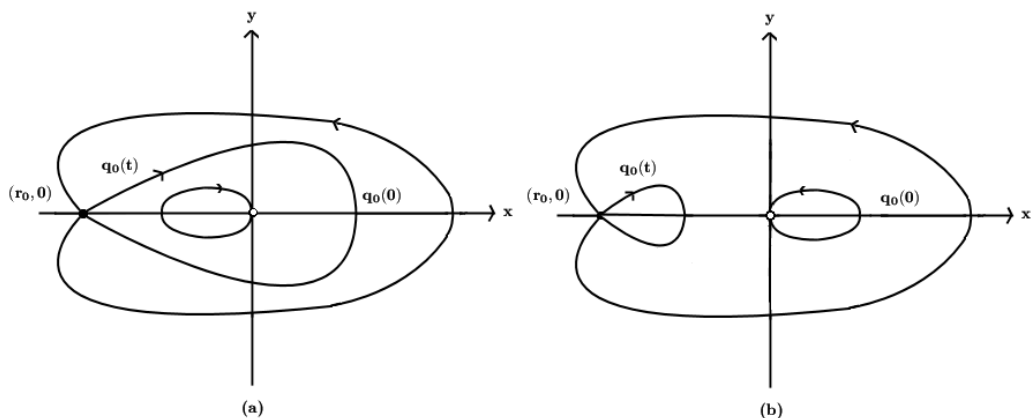


Figure 2: The homoclinic orbit $\mathbf{q}_0(t)$ for the cases (a) $\varphi_{bi}(\lambda) < \varphi < \varphi_{cr}(\lambda)$ and (b) $\varphi < \varphi_{bi}(\lambda)$ on axes $(x, y) = (r \cos \theta, r \sin \theta)$ with a singularity at $r = 0$.

The evolution of the elliptical dual domain $X(t)$ resembles the elliptical vortex patch studied by Bertozzi [3]. Theorem 1.4 in [20] shows that when $\lambda > 2$ and $\varphi < \varphi_{cr}(\lambda)$, there exist hyperbolic fixed points located symmetrically across from each other on the y -axis and connected by a heteroclinic saddle connection. In the coordinates $\theta = 2\hat{\theta}$ we have chosen to work in, this orbit becomes homoclinic and resembles the orbit shown in Figures 2 and 3. Moreover, there is a bifurcation curve $\varphi_{bi}(\lambda) < \varphi_{cr}(\lambda)$ separating two distinct phase space structures. For $\varphi > \varphi_{bi}(\lambda)$ we have the phase space of Figure 2(a) and for $\varphi < \varphi_{bi}(\lambda)$ the phase space resembles 2(b). In much the same way as in [3], the parameter s will be perturbed periodically and the Melnikov integral (7) will be evaluated along this orbit. Melnikov's theorem from section 1 will then be used to establish the chaotic response of the Hamiltonian vector field given by (16)–(17) to gentle periodic forcing in the flow regimes $\varphi < \varphi_{cr}(\lambda)$ given by,

$$\sinh \frac{\varphi_{cr}(\lambda)}{2} = \frac{1}{\lambda\sqrt{2}} \left(-1 + \sqrt{\frac{\lambda^2 - 1}{3}} \right)^{3/2}, \quad (18)$$

which contain this homoclinic orbit. We remark that when $\varphi = \varphi_{bi}(\lambda)$ the inner homoclinic orbit contains a singularity and this situation is dealt with by evaluating the Melnikov integral around the outer saddle connection connecting $(r_0, 0)$ to itself in Figure 2. The existence of the homoclinic saddle connection follows from the rigorous analysis of [20].

2.3 Three dimensional quasi-geostrophic ellipsoidal vortex patch.

Meacham et al [22] studied the 3D quasi-geostrophic equations in the case of

2 SOME EXACT SOLUTIONS TO THE SEMI-GEOSTROPHIC (SG)
AND QUASI-GEOSTROPHIC (QG) EQUATIONS

initial data corresponding to an ellipsoidal region $X(0) \subset \mathbf{R}^3$ with unit vorticity in the interior and zero vorticity outside, in the presence of a background stream function. The 3D quasi-geostrophic equations are obtained in exactly the same way as the semi-geostrophic equations are, with further approximation (15) of the advection operator in the inertial terms as was done for *SG* in equation (13). This additional approximation corresponds to replacing the coefficient $J\nabla\psi$ of D^2P with $J\nabla P$ in equation (13) in 2 dimensions, yielding (15), and is similar in \mathbf{R}^3 . We are mainly concerned here with the vorticity formulation and will direct the reader interested in understanding the *QG* model to [28]. Meacham et al [22] studied,

$$\left(\frac{\partial}{\partial t} + \left(-\frac{\partial\psi_T}{\partial y}, \frac{\partial\psi_T}{\partial x}\right) \cdot \nabla\right)\Delta\psi_T = 0 \quad (19)$$

where the total stream function ψ_T is decomposed into *endogenous* and *exogenously* controlled stream functions ψ and $\bar{\psi}$ respectively:

$$\psi_T := \psi + \bar{\psi}. \quad (20)$$

The *endogenous* stream function $\psi : \mathbf{R}^3 \rightarrow \mathbf{R}$ satisfies,

$$\Delta\psi = \mathbf{1}_{X(t)}, \quad (21)$$

$$X(0) = \{(x, y, z) \in \mathbf{R}^3 : \frac{x^2}{a^2} + \frac{y^2}{b^2} + \frac{z^2}{c^2} \leq 1\}. \quad (22)$$

The *exogenously* controlled stream function $\bar{\psi} : \mathbf{R}^3 \rightarrow \mathbf{R}$ corresponds to an externally controlled, vorticity free shearing field, defined as:

$$\bar{\psi}(x, y, z) = \frac{\lambda}{4}(x^2 + y^2) + \frac{s}{4}(x^2 - y^2) - \tau yz, \quad (23)$$

with control parameters $(\lambda, s, \tau) = (\lambda(t), s(t), \tau(t))$ representing an overall background rotation, the strength of a straining field, and the strength of a vertical shear respectively. A set of exact solutions to (19)–(23) were obtained by Meacham et al in [23] and were further studied by Meacham et al in [22]. There it was shown that the above equations are constrained to lie on a finite dimensional submanifold, where the ellipsoid $X(t)$ remains an ellipsoid of fixed volume and unit vorticity for all times. When $\tau = 0$, it was shown the equations had a canonical Hamiltonian structure in canonically conjugate variables (r, θ) where $r = \cosh \sigma$, with $e^\sigma = a/b$ and θ , which is $1/2$ the rotation of the ellipsoid in the plane corresponding to semi-minor and semi-major axes a, b . The explicit solution was found to be,

$$\frac{d}{dt} \begin{pmatrix} r \\ \theta \end{pmatrix} = J\nabla H_{QG}^{\lambda, s}(r, \theta), \quad (24)$$

$$H_{QG}^{\lambda, s}(r, \theta) = 2s\sqrt{r^2 - 1} \cos \theta - \lambda r + \int_0^r \Omega(t) dt, \quad (25)$$

$$\gamma := \left| \frac{s}{\lambda} \right| < 1 \text{ and } 0 < \gamma < \gamma_{cr}^{QG}$$

where $\Omega(t)$ is a rotation frequency dependent on the aspect ratio $a(t)/b(t)$ and for $\gamma \geq \gamma_{cr}^{QG}$, similar to the SG case, the above Hamiltonian is still well defined but does not contain a homoclinic orbit. The phase space corresponding to (25) was studied in [22] and is very similar to that of (17). It again possess a homoclinic fixed point on the x-axis connected by a homoclinic saddle connection as shown in Figure 3. Note also that both (25) and (17) are symmetric with respect to reflections across the x axis as a result of the $\cos \theta$ term in the Hamiltonian being the only angular dependence. This will be important in the analysis of the next section.

In the next section we exploit the symmetries present in the exact Hamiltonian solutions for both SG, QG and 2D Euler to simplify the Melnikov analysis in a similar way as was done in [3],[10],[16].

3 Chaotic Dynamics in Euler, SG, and QG.

3.1 Hamiltonian form of Bertozzi's equations. We now apply the Melnikov method to McCann and Oberman's [20] solutions of the semi-geostrophic equations, (16)–(17) as described in the previous section by introducing a time periodic perturbation of the domain eccentricity $s = \cosh \varphi$. Our calculation proceeds in much the same way as Bertozzi's [3] for the Kirchoff ellipse, who instead perturbed vortex patch eccentricity, but we use the Hamiltonian form of Melnikov's method which is simpler. In fact, by making the change of variables $a = e^{\frac{\sigma}{2}}$, $b = e^{-\frac{\sigma}{2}}$ and $r = \cosh \sigma$, the evolution equations for the elliptical vortex patch given by Bertozzi [3] become

$$\dot{a} - s \cos(2\tilde{\theta})a = 0, \tag{26}$$

$$\dot{b} + s \cos(2\tilde{\theta})b = 0, \tag{27}$$

$$\dot{\tilde{\theta}} = \frac{\lambda ab}{(a+b)^2} - s \frac{a^2 + b^2}{a^2 - b^2} \sin 2\tilde{\theta}, \tag{28}$$

where a, b are the semi major and semi minor axes of the ellipse, $\tilde{\theta}$ is the inclination with respect to the x axis, s is the principle rate of strain in the directions $x = \pm y$ and λ is the background rotation strength. We can cast these equations into a Hamiltonian system in the variables $(r(t), \theta(t)) := (\frac{\pi}{2} - 2\tilde{\theta})$,

$$\frac{d}{dt} \begin{pmatrix} r \\ \theta \end{pmatrix} = J \nabla H_{EL}^{\lambda,s}(r, \theta), \tag{29}$$

$$0 < \frac{s}{\lambda} < \gamma_{cr}^{EL}$$

$$H_{EL}^{\lambda,s}(r, \theta) = -2s\sqrt{r^2 - 1} \cos \theta + \lambda \log(r + 1), \tag{30}$$

where once again the Hamiltonian only possesses a homoclinic orbit for $0 < \frac{s}{\lambda} < \gamma_{cr}^{EL}$ but is well-defined outside of this regime. Here γ_{cr}^{EL} can be numerically calculated to be approximately 0.15 by solving for the real roots of the following equation

$$r^4 - 2r^3 + r^2 - 1 = 0 \quad (31)$$

$$\text{where } \gamma_{cr}^{EL} = \frac{1}{2r} \sqrt{\frac{r-1}{r+1}}. \quad (32)$$

Consequently, Bertozzi's result could have been obtained by exactly the same symmetry argument we use below with the Hamiltonian form of Melnikov's integral. Note that (30) shares the same symmetries as (17) for SG and (25) for QG, and once again has a homoclinic saddle connection with hyperbolic fixed point on the x-axis as shown in Figure 3.

3.2 Setting up the Melnikov integral. In this section we will denote the Hamiltonian as $H^{\lambda,s}$ when the equations apply to all three models, $H_{SG}^{\lambda,s}$, $H_{QG}^{\lambda,s}$ and $H_{EL}^{\lambda,s}$. We note that we work exclusively in the parameter ranges given below each Hamiltonian to ensure the existence of the homoclinic orbit. Equations (17), (25), (30) under a periodic perturbation of the parameter s can then be written as,

$$H^{\lambda,s_0+\epsilon \cos(kt+kt_0)}(r, \theta) := H^{\lambda,s_0}(r, \theta) + \epsilon \cos(kt+kt_0) \frac{\partial H^{\lambda,s}}{\partial s} \Big|_{s_0} (r, \theta) + O(\epsilon^2). \quad (33)$$

From this we can see that the gradient of the perturbed Hamiltonian, $H^{\lambda,s_0+\epsilon \cos(kt+kt_0)}$, can be written as,

$$\nabla H^{\lambda,s_0+\epsilon \cos(kt+kt_0)} = \nabla H^{\lambda,s_0} + \epsilon \cos k(t+t_0) \nabla \frac{\partial H^{\lambda,s}}{\partial s} \Big|_{s_0} + O(\epsilon^2). \quad (34)$$

Now the perturbed Hamiltonian vector field can be written as,

$$\frac{d}{dt} \begin{pmatrix} r \\ \theta \end{pmatrix} = \mathbf{f}(r, \theta) + \epsilon \mathbf{g}(r, \theta, t, \epsilon), \quad (35)$$

where $\mathbf{f} = J\nabla H^{\lambda,s_0}$, $\mathbf{g} = J\nabla \frac{\partial H^{\lambda,s}}{\partial s} \Big|_{s_0} \cos(kt+kt_0) + O(\epsilon)$. We note that in order to ensure \mathbf{g} satisfies the conditions of Melnikov's theorem (Theorem 1) we need only ensure that $\frac{\partial^2 H^{\lambda,s}}{\partial s^2}$ is smooth and bounded in our region of interest (which is indeed the case for all three Hamiltonians). We can now compute $\mathbf{f} \wedge \mathbf{g}$ in the Melnikov integral (7), noting that the (35) is of the form (7), with perturbed vector field:

$$\mathbf{f}(r, \theta) \wedge \mathbf{g}(r, \theta, t+t_0, 0) = \cos(kt+kt_0) J\nabla H^{\lambda,s_0}(r, \theta) \wedge J\nabla \frac{\partial H^{\lambda,s}(r, \theta)}{\partial s} \Big|_{s_0}. \quad (36)$$

Recall from section 2 that for $\varphi < \varphi_{cr}(\lambda)$ where $\varphi_{cr}(\lambda)$ satisfies (18), $H_{SG}^{\lambda,s}$ possesses a homoclinic saddle connection as shown in Figure 2. When $0 < |s/\lambda| < \gamma_{cr}^{EL} \simeq 0.15$ where γ_{cr}^{EL} solves (31)–(32), $H_{EL}^{\lambda,s}$ has a homoclinic fixed point lying on the x-axis outside of the unit disk as shown in Figure 3. Finally [22] show when $0 < \gamma := |s/\lambda| < \gamma_{cr}^{QG}$ for some $\gamma_{cr}^{QG} > 0$ that $H_{QG}^{\lambda,s}$ also has a homoclinic orbit as shown in Figure 3.

In all three cases, we denote the time parametrization of this orbit as $\mathbf{q}_0(t) = (r(t), \theta(t))$ with $\mathbf{q}_0(0)$ lying on the x-axis as shown in Figures 2 and 3. Since $H^{\lambda,s}(r, -\theta) = H^{\lambda,s}(r, \theta)$ (for $H_{SG}^{\lambda,s}, H_{QG}^{\lambda,s}$ and $H_{EL}^{\lambda,s}$), it follows that $\mathbf{f} \wedge \mathbf{g}(\mathbf{q}_0(t), t, 0) = -\mathbf{f} \wedge \mathbf{g}(\mathbf{q}_0(-t), t, 0)$ from (36). For $t_0 \in \mathbf{R}$, we then seek to evaluate,

$$M(t_0) = \int_{-\infty}^{\infty} \mathbf{f}(\mathbf{q}_0(t)) \wedge \mathbf{g}(\mathbf{q}_0(t), t + t_0, 0) dt. \quad (37)$$

3.3 Main results. We show below that the Melnikov integral defined by equations (34), (35) has simple zeros for all but countably many perturbation frequencies $k \in \mathbf{R}$, for $H_{SG}^{\lambda,s}, H_{QG}^{\lambda,s}$ and $H_{EL}^{\lambda,s}$. Melnikov’s theorem combined with the Smale-Birkhoff theorem then allow us to conclude the presence of chaotic dynamics in a neighborhood of the hyperbolic saddle connection shown in Figures 2,3.

Our method of proof involves exploiting the fact that the fourier transform of an exponentially decaying function is analytic. The Melnikov integral defined by equations (34), (35) will be shown to be the fourier transform of a function involving gradients of $H^{\lambda,s}$ and $\frac{\partial H^{\lambda,s}}{\partial s}$, parameterized along the orbit in Figure 3. Since the Melnikov integral measures the leading order separation of W^s and W^u , this will guarantee transversal intersections as long as the integral (34) doesn’t vanish identically, which is checked for each of the three fluid models in section 4 (appendix). We first establish the following lemma which will prove useful for our main result; it shows that $\nabla H^{\lambda,s}(\mathbf{q}_0(t))$ does indeed decay exponentially as $t \rightarrow \pm\infty$. We work in a general setting however since the result is a general consequence of the asymptotic stability of the stable manifolds to hyperbolic fixed points. This result is well known [11], [31] but we include the proof for the two dimensional case for completeness.

Lemma 3 *Let $\dot{\mathbf{x}} = \mathbf{f}(\mathbf{x})$ be an ODE on a smooth 2-manifold \mathcal{M} with $\mathbf{f} : \mathcal{M} \rightarrow \mathcal{T}\mathcal{M}$ smooth. If \mathbf{x}_0 is a homoclinic fixed point then $\mathbf{f}(\mathbf{x}(t))$ decays exponentially as $t \rightarrow \pm\infty$ where $\mathbf{x}(t)$ parameterizes the homoclinic saddle orbit to \mathbf{x}_0 .*

Proof: We first recall the definitions for stable and unstable manifolds for a fixed point \mathbf{x}_0 of a continuous time flow $\mathbf{x}(t)$ induced by $\dot{\mathbf{x}} = \mathbf{f}(\mathbf{x})$:

$$W^s := \{\mathbf{y} \in \mathcal{M} : \mathbf{x}(t) \rightarrow \mathbf{x}_0 \text{ as } t \rightarrow \infty, \mathbf{x}(0) = \mathbf{y}\},$$

$$W^u := \{\mathbf{y} \in \mathcal{M} : \mathbf{x}(t) \rightarrow \mathbf{x}_0 \text{ as } t \rightarrow -\infty, \mathbf{x}(\mathbf{0}) = \mathbf{y}\}.$$

We set $\mathbf{x}_0 = 0$ without loss of generality and note that homoclinic orbits on a 2-manifold are always hyperbolic. The stable manifold theorem [11] then tells us that the stable and unstable manifolds of the *linearized* system $\dot{\mathbf{x}} = D\mathbf{f}(\mathbf{0})\mathbf{x}$, denoted \mathcal{E}^s and \mathcal{E}^u , form the tangent space to W^s and W^u respectively at $\mathbf{0}$, both of which are smooth manifolds. Hence we can restrict the ODE to a local neighborhood of $\mathbf{0}$ in W^s with tangent space \mathcal{E}^s and guarantee the solutions remain in this set for all forward times by the stability of the manifold. All subsequent calculations assume this restriction. Now work in a local coordinate chart in this subset of the manifold. Since \mathbf{f} is smooth we can do a Taylor expansion about the point $\mathbf{x}_0 = 0$,

$$\dot{\mathbf{x}} = D\mathbf{f}(\mathbf{0})(\mathbf{x}) + R(\mathbf{x}),$$

where $R(\mathbf{x})$ is a remainder term containing terms of order $|\mathbf{x}|^2$ and higher and $|\cdot|$ represents the Euclidian metric on the coordinates. Now let $\mathbf{x}(t)$ be any curve lying on W^s that solves the ODE. Differentiating $|\mathbf{x}(t)|^2$ with respect to time we obtain,

$$\frac{d|\mathbf{x}(t)|^2}{dt} = 2\langle \dot{\mathbf{x}}(t), \mathbf{x}(t) \rangle \quad (38)$$

$$= 2\langle \mathbf{f}(\mathbf{x}(t)), \mathbf{x}(t) \rangle \quad (39)$$

$$= 2\langle D\mathbf{f}(\mathbf{0})\mathbf{x}(t) + R(\mathbf{x}(t)), \mathbf{x}(t) \rangle \quad (40)$$

$$\leq -2c|\mathbf{x}(t)|^2 + 2|R(\mathbf{x}(t))| \cdot |\mathbf{x}(t)|. \quad (41)$$

Where $c > 0$ is smaller in absolute values than all of the eigenvalues of $D\mathbf{f}(\mathbf{0})$, which are negative since we are on a stable manifold. Since R has $O(|\mathbf{x}|^2)$ control we can choose a $T > 0$ so that

$$|R(\mathbf{x}(t))| \leq \frac{c}{2}|\mathbf{x}(t)|.$$

Then we conclude that

$$\frac{d|\mathbf{x}(t)|^2}{dt} \leq -c|\mathbf{x}(t)|^2.$$

Hence all coordinates of $\mathbf{x}(t)$ decay exponentially and so by Taylor expanding $\mathbf{f}(\mathbf{x})$ about $\mathbf{x}_0 = \mathbf{0}$, we can conclude that $\mathbf{f}(\mathbf{x}(t)) \rightarrow 0$ exponentially as $t \rightarrow \infty$. The argument is the same under time reversal due to the fixed point being homoclinic. \square

We now recall a second Lemma which allows us to use exponential decay of a function as a sufficient condition for analyticity in an open subset of the complex plane given e.g by Dym and McKean [21]. We include the proof for the sake of completeness. Since we will show that the Melnikov integral can be written as (47), the existence of simple zeroes will be guaranteed since the integral in (47) will vanish for no more than countably many perturbation frequencies $k \in \mathbf{R}$. Below $\hat{f}(k)$ denotes the fourier transform (42) of $f : \mathbf{R} \rightarrow \mathbf{R}$.

Lemma 4 *Given $f : \mathbf{R} \rightarrow \mathbf{R}$, if there exists $T, B > 0$ such that $|f(t)| \leq \text{constant} \times e^{-B|t|}$ for all $|t| > T$ and $f(t) \leq M < \infty$ for all $t \in \mathbf{R}$, then $\hat{f}(k)$ is analytic in the open strip $U := \{\gamma = a + ib : |2\pi b| < B\}$.*

Proof: Any differentiable complex-valued function that satisfies the Cauchy-Riemann equations is well known to be analytic. Hence our first goal is to verify the fourier transform of the function $f : \mathbf{R} \rightarrow \mathbf{R}$ is differentiable. This involves differentiating under the integral and hence requires the Lebesgue dominated convergence theorem. Secondly we must verify the function satisfies that the Cauchy Riemann equations.

First recall the fourier transform of a function $f : \mathbf{R} \rightarrow \mathbf{R}$ is defined as

$$\hat{f}(k) := \int_{-\infty}^{\infty} f(t)e^{-2\pi ikt} dt. \quad (42)$$

Write $k = a + bi$ where $a, b \in \mathbf{R}$. Then

$$\hat{f}(a + bi) = \int_{-\infty}^{\infty} f(t)e^{-2\pi(a+bi)it} dt \quad (43)$$

$$= \int_{-\infty}^{\infty} f(t) \cos(2\pi at)e^{2\pi bt} - i \int_{-\infty}^{\infty} f(t) \sin(2\pi at)e^{2\pi bt} dt \quad (44)$$

$$=: u(a + bi) + iv(a + bi) \quad (45)$$

using Euler's identity.

Now we verify differentiability of $\hat{f}(k)$. Differentiating with respect to a , we get the following estimate for the integrand:

$$\left| \frac{\partial}{\partial a} f(t) \cos(2\pi at)e^{2\pi bt} \right| \leq C e^{-B|t|} |2\pi t| e^{2\pi bt} \in L^1(\mathbf{R}; dt)$$

where $|t| > T$, provided $|2\pi b| < B$. We can now apply the dominated convergence theorem to differentiate (43) under the integral sign with respect to a using the above bound. A similar argument shows we can differentiate (43) with respect to b . It follows that $\hat{f}(k) \in C^1(\mathbf{R}^2; \mathbf{R}^2)$. Lastly, it is easily checked that $\frac{\partial u}{\partial a} = \frac{\partial v}{\partial b}$ and $\frac{\partial u}{\partial b} = -\frac{\partial v}{\partial a}$ and hence the Cauchy-Riemann equations are satisfied for u, v in $U := \{\gamma = a + ib : |2\pi b| < B\}$. Consequently, $\hat{f}(k)$ is analytic in U . \square

We now prove our main result, which shows that the Melnikov integral, defined by (36), (37) has simple zeros for all but countably many periods. Melnikov's theorem combined with the Smale-Birkhoff theorem for homoclinic orbits then allows us to conclude the presence of chaotic dynamics for initial conditions in a neighborhood of the fixed point $(r_0, 0)$ shown in Figure 3.

Theorem 5 *The Melnikov function $M(t_0)$ defined by (36), (37) has simple zeros $M(0) = 0 \neq M'(0)$ for all perturbation frequencies $k \in \mathbf{R}$ outside a set $K \subset \mathbf{R}$ which has no accumulation points. In particular, the set K of exceptional frequencies is countable.*

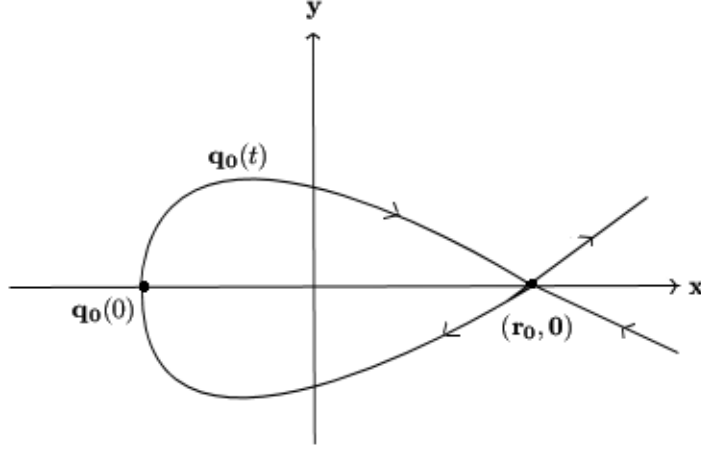


Figure 3: Homoclinic orbit $\mathbf{q}_0(t)$ possessed by $H_{EL}^{\lambda,s}, H_{QG}^{\lambda,s}$ with fixed point $(r_0, 0)$

Proof: Combining equations (35) and (36) gives us the following equation for the Melnikov function,

$$M(t_0) = \int_{-\infty}^{\infty} J\nabla H^{s,\lambda}(\mathbf{q}_0(t)) \wedge J\nabla \frac{\partial H^{s,\lambda}(\mathbf{q}_0(t))}{\partial s} \Big|_{s_0} \cos(kt + kt_0) dt.$$

Defining

$$\begin{aligned} \mathbf{f} \wedge \mathbf{g}(\mathbf{q}_0(t)) &= J\nabla H^{s,\lambda}(\mathbf{q}_0(t)) \wedge J\nabla \frac{\partial H^{s,\lambda}(\mathbf{q}_0(t))}{\partial s} \Big|_{s_0} \cos(kt + kt_0) \\ &=: f(t) \cos(kt + kt_0) \end{aligned} \quad (46)$$

we see from the reflection symmetry of H_{SG} in (17), H_{QG} in (25), and H_{EL} in (30) across the x -axis (see Figure 3), that the cross product term, $f(t)$, satisfies $f(-t) = -f(t)$. Rewriting $\cos(t+t_0)k$ as $\cos(kt)\cos(kt_0) - \sin(kt)\sin(kt_0)$, note that the even part of the Melnikov integral vanishes as one integrates over \mathbf{R} . Consequently,

$$M(t_0) = \sin(kt_0) \int_{-\infty}^{\infty} \sin(kt) f(t) dt. \quad (47)$$

Note that $f(t)$ is written entirely in terms of gradients of H . Lemma 1 immediately yields that $f(t)$ decays exponentially as $t \rightarrow \pm\infty$, and is clearly bounded since all of our Hamiltonians are smooth within our region of interest except for the case where $r = 1$ on the orbit in (30) which Bertozzi [3] deals with by working in cartesian coordinates. The homoclinic orbit shown in Figure 2 incurs a singularity when $\varphi = \varphi_{bi}(\lambda)$, the bifurcation curve separating the regimes in Figure 2, however we can simply choose the outer homoclinic orbit in Figure 2

in this case and so the case $\varphi = \varphi_{bi}(\lambda)$ is included in our result. We can now use Lemma 2, which tells us that the fourier transform of a function that decays exponentially is analytic in an open neighborhood of the complex plane containing the real line ($b = 0$ where $z = a + bi$). From Corollary 8 (see appendix), we see that $f(t)$ is not identically zero for H_{SG} , H_{QG} and H_{EL} . Hence the real zeros of the fourier transform, $\hat{f}(k)$ cannot accumulate. It follows that for all but countably many $k \in \mathbf{R}$, $M(t_0)$ has simple zeros since $\sin(kt_0)$ does (eg. at $t_0 = 0$). \square

Remark 6 *Note that if we perturb the potential vorticity λ instead of the domain eccentricity s in H_{SG} , a similar conclusion holds, but the calculations are simpler since the dependence of $H_{SG}^{\lambda, s}$ on λ is much simpler.*

4 Discussion and conclusions

In the context of this paper, chaos can be understood to mean sensitivity of the dynamics to initial conditions, or more specifically, topological conjugacy of a subset of the dynamics to the bi-infinite shift on two symbols. This mathematics underlies what is popularly known as the butterfly effect. Bertozzi [3] and subsequent authors have demonstrated that certain elliptical vortex patch solutions of the 2D Euler equations become chaotic in this sense when small-amplitude time-periodic perturbations are introduced in the form of a background shearing field. Our analysis simplifies her argument and strengthens her conclusions, by showing this chaotic response occurs not only in a positive interval of perturbation frequencies, but at all such frequencies outside of a countable, topologically isolated set.

Using the same technique, we confirm a similar chaotic response to a gently oscillating shear field observed numerically by Meacham et al for an elliptical potential vortex patch evolving as 3D quasi-geostrophic fluid [22], and of 2D semi-geostrophic fluid rotating in an elliptical tank to gentle periodic perturbations of the tank's eccentricity. These results are of interest because the quasi-geostrophic and semi-geostrophic dynamics are examples of balanced models: they approximate the primitive equations governing rotating fluids in the atmosphere and oceans (gravitationally stratified in the 3D case), by using a separation of time scales to assume pressure gradients instantaneously adjust to balance the Coriolis force of rotation, and to maintain gravitational stratification in 3D. There is considerable evidence for the stabilizing effects of rotation and stratification in fluids, and one might naively hope the instabilities in the primitive equations are due to the rapid but non-instantaneous response to imbalance, and might therefore be absent from the balanced models, enabling the latter to produce longer, more stable, and reliable forecasts. On the contrary, our analysis shows the chaotic response of elliptical potential vorticity patches in the balanced models to be remarkably similar to that of the 2D Euler equation. The mathematical similarity seems to us somewhat surprising since the equa-

tions model different physics: the 2D Euler equation, if viewed as a balanced model, would model motion independent of depth on small horizontal scales, whereas the semi-geostrophic equation models motion independent of the depth on large horizontal scales. But the chaotic response of the balanced models is made less surprising after observing that it occurs in a flow regime outside the realm of validity of the semi-geostrophic and quasi-geostrophic approximations: the semi-geostrophic equations, in particular, are not expected to be accurate for large values $\lambda \gg 1$ of inverse potential vorticity [6].

Acknowledgements

The authors would like to thank Professor Phillip J. Morrison for suggesting this problem, and Professors Mary Pugh, Philip Holmes, Charles Pugh and Michael Cullen for fruitful discussions during the course of this work. We are grateful to the United States National Science Foundation grant DMS 0354729, Natural Sciences and Engineering Research Council of Canada grant 217006-03 RGPIN, the University of Toronto Excellence Award (UTEA) in the Natural Sciences and Engineering, held during the summer of 2006 and an NSERC Undergraduate Student Research Award (USRA) held during the summer of 2007.

A Appendix

The purpose of this appendix is to ensure that the cross product term $f(t)$, as defined by equation (41), does not vanish identically for any of the Hamiltonians (17), (25), (30). This is necessary in the proof of Theorem 4 to ensure that $f(t)$ is non-zero at all but a countable, topologically isolated set of points. We accomplish this goal by first proving a technical lemma which amounts to verifying that the level sets of $H^{\lambda,s}$ and $\frac{\partial H^{\lambda,s}}{\partial s}$ are not coincident along the entire saddle connection $\mathbf{q}_0(t)$ in Figure 3.

Lemma 7 *Given H defined by (17), (25), (30), if $(r, 0) \in \mathbf{R}^2$ is the homoclinic fixed point of H in figures 2 and 3 and*

$$(1) \frac{\partial^2 H^{\lambda,s}}{\partial s \partial \theta}(r, 0) = 0,$$

$$(2) \frac{\partial^2 H^{\lambda,s}}{\partial s \partial r}(r, 0) \neq 0,$$

then we have that $\nabla H^{\lambda,s}(\mathbf{q}_0(t)) \wedge \nabla \frac{\partial H^{\lambda,s}}{\partial s}(\mathbf{q}_0(t)) \neq 0$ for some $t \in \mathbf{R}$.

Proof: We inspect local behavior around the homoclinic fixed point $(r, 0)$ and demonstrate that the contours of $H^{\lambda,s}$ and $\frac{\partial H^{\lambda,s}}{\partial s}$ are not parallel. Conditions (1) and (2) above allow us to conclude that the level set of $\frac{\partial H^{\lambda,s}}{\partial s}$ passing through the point $(r, 0)$ intersects the x-axis at an angle of $\pi/2$. It was shown in [20] that the fixed point $(r, 0)$ for H_{SG} is non-degenerate, meaning $\det[D^2 H_{SG}^{\lambda,s}(r, 0)] \neq 0$. The fixed points are shown to be non-degenerate for $H_{QG}^{\lambda,s}$ in [23]. Bertozzi [3] makes use of the fact that the fixed point is hyperbolic, and this can be seen

easily by computing

$$\det[D^2 H_{EL}^{\lambda,s}(r, 0)] = s\sqrt{r^2 - 1} \left(\frac{1}{(r+1)^2} + \frac{s}{2(r^2 - 1)} \right) \neq 0,$$

when $r > 1$. We also see from a simple calculation that $\frac{\partial H^{\lambda,s}}{\partial r \partial \theta}(r, 0) = 0$ for all three Hamiltonians and hence the matrix $D^2 H^{\lambda,s}$ is diagonalized in these coordinates at the fixed point. This, combined with the non-vanishing of the determinant ensures that the saddle connection of the unperturbed Hamiltonians will not intersect the x-axis at an angle of $\pi/2$. The implicit function theorem therefore ensures that in a local neighborhood of the fixed point, the contours of $H^{\lambda,s}$ and $\frac{\partial H^{\lambda,s}}{\partial s}$ are not parallel due to the non-degeneracy of the fixed point (the contours of $H^{\lambda,s}$ appear as in Figure 3). Hence there must exist a point on $\mathbf{q}_0(t)$ near $(r, 0)$ where $\nabla H^{\lambda,s}$ and $\nabla \frac{\partial H^{\lambda,s}}{\partial s}$ are not parallel, and hence a point where $\nabla H^{\lambda,s}(\mathbf{q}_0(t)) \wedge \nabla \frac{\partial H^{\lambda,s}}{\partial s}(\mathbf{q}_0(t)) \neq 0$. \square

We now proceed with the calculations:

Corollary 8 *The cross product term, $f(t)$, defined by (42) is non-zero for some $t \in \mathbf{R}$ for H_{QG} , H_{SG} and H_{EL} .*

Proof: We complete the proof by breaking it down into three cases, for the Hamiltonians H_{QG} , H_{EL} and H_{SG} defined by equations (25), (30), and (17) respectively.

Case 1: Quasi-geostrophic vortex patch.

We must show that

$$\nabla H_{QG}^{\lambda,s}(\mathbf{q}_0(t)) \wedge \nabla \frac{\partial H_{QG}^{\lambda,s}}{\partial s}(\mathbf{q}_0(t)) \neq 0 \text{ for some } t \in \mathbf{R}. \quad (48)$$

Lemma 6 gives us three conditions that we can verify that are sufficient to yield this result.

Differentiating (25) with respect to the parameter s gives,

$$\frac{\partial H_{QG}^{\lambda,s}}{\partial s} = -\frac{1}{2}\sqrt{r^2 - 1} \cos \theta.$$

Differentiating with respect to θ clearly gives $\frac{\partial H_{QG}^{\lambda,s}}{\partial s \partial \theta} = 0$ at the point $\theta = 0$, but

$$\frac{\partial^2 H_{QG}^{\lambda,s}}{\partial s \partial r} = \frac{-1}{2} \frac{r \cos \theta}{\sqrt{r^2 - 1}},$$

which does not vanish where r is defined and $\theta = 0$. By choosing $r = r_0$ to be the homoclinic fixed point that H possesses, we have that conditions (1), (2), (3)

in Lemma 6 are satisfied and the result follows.

Case 2: Kirchoff elliptical vortex patch.

Proof: The argument is exactly the same as it was for QG because of the similarity of the Hamiltonians H_{QG} and H_{EL} and we refer the reader to case 1 for the calculation. \square

Case 3: Semi-geostrophic vortex patch.

Proof: This calculation is more laborious than for H_{EL} and H_{QG} . We define

$$z(r, \theta; s) = \sqrt{2} \sqrt{1 + rs + \sqrt{(r^2 - 1)(s^2 - 1)} \cos \theta}, \quad (49)$$

Differentiating (17) with respect to the parameter s gives,

$$\begin{aligned} \frac{\partial H_{SG}^{\lambda, s}}{\partial s} &= 2\lambda^2 - \frac{\lambda}{z} \frac{\partial}{\partial s} \left(z^2 \right) \\ &= 2\lambda^2 - \frac{\lambda}{z} \left[2r + 2s \cos \theta \sqrt{\frac{r^2 - 1}{s^2 - 1}} \right] \end{aligned} \quad (50)$$

Now

$$\frac{\partial^2 H_{SG}^{\lambda, s}}{\partial s \partial r} = -\lambda \frac{\partial}{\partial r} \left[\frac{r + s \cos \theta \sqrt{\frac{r^2 - 1}{s^2 - 1}}}{z} \right] \quad (51)$$

We wish to determine under what conditions $\frac{\partial^2 H_{SG}^{\lambda, s}}{\partial s \partial r}(r, \pi) = 0$. So we find the zeros of (51) with $\theta = \pi$,

$$z \left(1 - \frac{rs}{\sqrt{(r^2 - 1)(s^2 - 1)}} \right) - \frac{1}{z} \left(r - s \sqrt{\frac{r^2 - 1}{s^2 - 1}} \right) \left(s - r \sqrt{\frac{s^2 - 1}{r^2 - 1}} \right) = 0 \quad (52)$$

Upon substituting $r = \cosh(\sigma)$ and $s = \cosh(\varphi)$, we obtain the equation

$$2(1 + \cosh(\sigma - \varphi)) \cosh(\sigma - \varphi) = \sinh^2(\sigma - \varphi) \quad (53)$$

Using $\cosh^2(\sigma - \varphi) - \sinh^2(\sigma - \varphi) = 1$ yields

$$2 \cosh(\sigma - \varphi) + 1 + \cosh^2(\sigma - \varphi) = 0$$

which finally gives,

$$(\cosh(\sigma - \varphi) + 1)^2 = 0. \quad (54)$$

Now (54) has no solutions and so choosing $r = r_0$ to be the fixed point of $H_{SG}^{\lambda, s}$ on the x-axis, conditions (1), (2), (3) in Lemma 6 are satisfied for $H_{SG}^{\lambda, s}$ and hence the result follows. \square

References

- [1] V I. ARNOLD. Sur la geometrie differentielle des groupes de Lie de dimension infinie et ses applications a l'hydrodynamique des fluides parfaits. *Ann. Inst. Fourier* **16** (1966) 316–361.
- [2] V I. ARNOLD. Instability of dynamical systems with several degrees of freedom. *Soviet Math. Dokl.* **5** (1965) 581–585.
- [3] A. BERTOZZI. Heteroclinic orbits and chaotic dynamics in planar fluid flows. *SIAM J. Math. Anal.* **19** (1988) 1271–1294.
- [4] G.D BIRKHOFF. Nouvelles recherches sur les systèmes dynamiques. *Pont. Acad. Sci. Novi Lyncaei* **1** (1935) 85–216.
- [5] M.J.P CULLEN & R.J PURSER. An extended Lagrangian theory of semi-geostrophic frontogenesis. *J. Atmos. Sci.* **41** (1984) 1477–1497.
- [6] M.J.P CULLEN. Large-scale non-turbulent dynamics in the atmosphere. *Quart. J. Royal Meteorol. Soc* **128** (2002) 241–73.
- [7] M.J.P CULLEN. A mathematical theory of large-scale atmosphere/ocean flow. *Imperial College Press, Met Office, UK* (2006).
- [8] M.J.P CULLEN, R J PURSER, G J SHUTTS. Modelling the quasi-equilibrium dynamics of the atmosphere. *Quart. J. Royal Meteorol. Soc* **113** (1987) 735–57.
- [9] M.J.P CULLEN & R.J DOUGLAS. Large-amplitude nonlinear stability results for atmospheric circulations. *Quart. J. Royal Meteorol. Soc* **129** (2003) 1969–1988.
- [10] P.J. HOLMES & H. DANKOWICZ. The existence of transverse homoclinic points in the Sitnikov problem. *J. Differential Equations.* **116** (1995) 468–483.
- [11] J. GUCKENHEIMER & P.J HOLMES. Nonlinear Oscillations, Dynamical Systems, and Bifurcations of Vector Fields. *Springer-Verlag, New York* (1983).
- [12] E.N. LORENZ. Deterministic nonperiodic flow. *J. Atmospheric Sci.* **20** (1963). 130–141.
- [13] P.J. HOLMES & J.E. MARSDEN. A partial differential equation with infinitely many periodic orbits: chaotic oscillations of a forced beam. *Arch. Ration. Mech. Anal.* **76** (1981) 135–166.
- [14] P.J. HOLMES & J.E. MARSDEN. Horseshoes in perturbations of hamiltonian systems with two degrees of freedom. *Commun. Math. Phys.* **82** (1982) 523–544.
- [15] P.J. HOLMES & J.E. MARSDEN. Melnikov's method and Arnold diffusion for perturbations of integrable Hamiltonian systems. *J. Math. Phys.* **23** (1982) 669–675.
- [16] P.J. HOLMES & J.E. MARSDEN. Horseshoes and Arnold diffusion for Hamiltonian systems on lie groups. *Indiana Univ. Math. J.* **32** (1983) 273–309.
- [17] P.J. HOLMES. Poincaré, celestial mechanics, dynamical-systems theory and “chaos”. *Phys. Reports* **193** (1990) 137–163.

- [18] S. KIDA Motion of an elliptic vortex in a uniform shear flow. *J. Phys. Soc. Japan* **50** (1981) 3517.
- [19] G. KIRCHOFF Vorlesungen über mathematische Physik. Mechanik. *Leipzig, 2nd edition* (1877)
- [20] R.J. MCCANN & A. OBERMAN. Exact semi-geostrophic flows in an elliptical ocean basin. *Nonlinearity* **17** (2004) 1891–1922.
- [21] H.P. MCKEAN & H. DYM. Fourier Series and Integrals. *Academic Press, New York* (1972).
- [22] S.P. MEACHAM & P.J. MORRISON & G.R. FLIERL. Hamiltonian moment reduction for describing vortices in shear. *Phys. Fluids* **9** (1997) 2310–2328.
- [23] S.P. MEACHAM & K.K. PANKRATOV, A.S. SHCHEPETKIN, V.V. ZHMUR. Ellipsoidal vortices in background shear and strain flows. *Dyn. Atmos. Oceans* **21** (1994) 167–212.
- [24] V.K MELNIKOV. On the stability of the center for time periodic perturbations. *Trans. Moscow Math. Soc.* **12** (1963) 1–57.
- [25] S.P. MEACHAM & P.J. MORRISON & K. NGAN. Elliptical Vortices in Shear: Hamiltonian moment formulation and Melnikov analysis. *Phys. Fluids* **8** (1996) 896–912.
- [26] J.C. NEU. The dynamics of a columnar vortex in an imposed strain.. *Phys. Fluids* **27** (1984) 2397-2402.
- [27] H. POINCARÉ. Sur les équations de la dynamique et let problème des trois corps. *Acta Math.* **13** (1890) 1–279.
- [28] R. SALMON. Geophysical Fluid Dynamics. *Oxford University Press, New York* (1998) pp. 63–80.
- [29] S. SMALE. Diffeomorphisms with many periodic points. *Differential Combinatorial Topology, S.S Cairns, ed., Princeton University Press, Princeton NJ* (1963) pp. 63–80.
- [30] G. TESCHL. Ordinary Differential Equations and Dynamical Systems. <http://www.mat.univie.ac.at/gerald/ftp/book-ode/>, Vienna (2001).
- [31] S. WIGGINS. Introduction to Applied Nonlinear Dynamical Systems and Chaos. *Springer-Verlag, New York* (2003).